MRI of Brain Disease in Veterinary Patients Part 1: Basic Principles and Congenital Brain Disorders

Silke Hecht, Dr Med Vet*, William H. Adams, DVM

KEYWORDS

• Magnetic resonance imaging • Brain • Dog • Cat
• Basic principles • Congenital disorders

Magnetic resonance imaging (MRI) is the imaging modality of choice in the diagnosis of brain diseases in human patients and is increasingly available in veterinary practice.[1,2] Advantages of MRI over computed tomography (CT) include improved contrast resolution, capabilities in multiplanar image acquisition, availability of specialized sequences, and use of nonionizing radiation. Disadvantages include longer acquisition time and less spatial resolution compared with CT. Although CT might be preferred to MRI in cases of acute head trauma where evaluation of small bony structures and minimization of anesthesia time are crucial, MRI is the superior imaging modality in the evaluation of most intracranial disorders.

BASIC MRI PRINCIPLES

In-depth review of MR physics is beyond the scope of this article. A short overview of basic principles is provided as a basis for understanding pulse sequences and appearance of pathologic changes on MR images. Diagnostic MRI images hydrogen protons, which are ubiquitous in biologic tissues.[3,4] As most pathologic processes result in the alteration of content, distribution, and ambient environment of hydrogen protons of tissues, MRI is an appropriate and sensitive modality for imaging of disease. When a patient is placed in an MR scanner, the hydrogen protons align along the main magnetic field. An excitation radiofrequency pulse is applied, which changes

Department of Small Animal Clinical Sciences, University of Tennessee College of Veterinary Medicine, 2407 River Drive, Knoxville, TN 37996, USA
* Corresponding author.
E-mail address: shecht@utk.edu (S. Hecht).

Vet Clin Small Anim 40 (2010) 21–38
doi:10.1016/j.cvsm.2009.09.005 **vetsmall.theclinics.com**
0195-5616/09/$ – see front matter

the energy state of the protons and results in their misalignment with the main magnetic field. As the protons return to their original energy level and realign with the main magnetic field, radiofrequency energy is emitted, creating a signal that is detected by a receiver coil. From its highest initial intensity immediately following excitation, the signal fades because of 2 simultaneous processes: The hydrogen protons align again with the main magnetic field (spin-lattice relaxation; T1 relaxation), and protons interfere with each other resulting in loss of transverse magnetization (spin-spin relaxation; T2 relaxation).[5,6] Differences in relaxation times of different tissues create differences in signal intensity emitted by tissues, resulting in tissue contrast. In general terms, water (pure fluid) has long relaxation times, various soft tissues have intermediate relaxation times, and fat has short relaxation times. Other contrast parameters intrinsic to individual tissues are the proton density, flow, and apparent diffusion coefficient (ADC).[3,4]

MRI SEQUENCES

MRI sequences are designed to acquire information by exploiting differences in behavior of hydrogen protons in varied tissues in changing magnetic fields.[4] MRI technology is constantly evolving, and more and varied sequences are becoming available. Commonly used MRI sequences for brain imaging include T1-weighting (T1-W, pre- and postcontrast), T2-weighting (T2-W), fluid attenuated inversion recovery (FLAIR), and T2*-weighting (T2*-W). Proton density weighting (PD-W), diffusion-weighted imaging (DWI), perfusion-weighted imaging (PWI), fat suppression techniques (short tau inversion recovery [STIR] and chemical fat suppression [fat saturation (FatSat)]), and ultrafast spin echo (SE) sequences. Magnetic resonance angiography (MRA), high-resolution sequences, and dynamic studies are less commonly performed but may be considered for certain indications. At the time of writing, functional MRI, diffusion tensor tractography, magnetization transfer imaging, and MR spectroscopy are not routinely performed in veterinary patients and are discussed elsewhere.[3,4,7,8]

T1-W

On T1-W images, contrast between tissues depends predominantly on differences in T1 relaxation times. Fat has short T1 relaxation time and is hyperintense, whereas fluid has long T1 relaxation time and appears hypointense. Soft tissues have somewhat variable intermediate T1 relaxation times and have medium intensity. After uptake of administered paramagnetic contrast agents, physiologically, contrast-enhancing tissues (eg, pituitary gland) and contrast-enhancing pathologic lesions (eg, certain brain tumors) are hyperintense (**Fig. 1**).[3,4]

T2-W

On T2-W images, contrast between tissues depends predominantly on differences in T2 relaxation times. Fluid and tissues with increased fluid content (“juicy tissues”) appear strongly hyperintense.[9] Intensity of fat is variable. A T2-W image can be considered a “pathology” scan, because abnormal fluid collections and tissues with abnormal increased fluid content (edema, inflammation, neoplasia, and so forth) will appear hyperintense (**Fig. 2**).[3,4,10]

FLAIR

FLAIR images are useful in conjunction with T2-W images in evaluating and characterizing T2 hyperintense lesions. Using FLAIR, pure fluid (cerebrospinal fluid [CSF] and

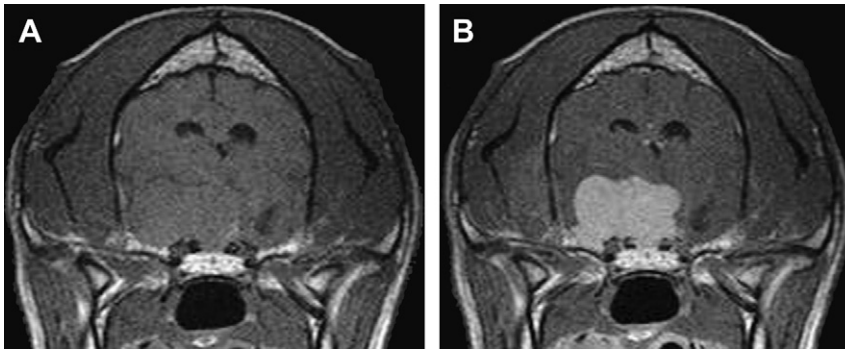

Fig. 1. Transverse T1-W images of a 9-year-old golden retriever pre- (*A*) and postadministration (*B*) of contrast medium. Fat associated with the subcutaneous tissues and bone marrow is hyperintense, and fluid (cerebrospinal fluid [CSF] within ventricles) is hypointense. A large intracranial mass (meningioma) is present, which is isointense to brain parenchyma on precontrast image and hyperintense on postcontrast image. Note mass effect (midline shift and compression of right lateral ventricle) on precontrast image.

fluid in cystic lesions) is suppressed and becomes hypointense, whereas solid lesions remain hyperintense, facilitating differentiation (**Fig. 3**). Additionally, this sequence increases conspicuity of small lesions bordering a fluid-filled ventricle or subarachnoid space (**Fig. 4**).[2,11,12] Without modification of acquisition parameters, FLAIR is unable to suppress the signal from fluids containing high protein, cell components, or blood by-products, a potential pitfall when interpreting images.[9,13] FLAIR images were initially exclusively acquired before contrast administration. However, postcontrast FLAIR images are very sensitive in the detection of contrast-enhancing lesions and may be used as an alternative to postcontrast T1-W imaging.[14]

T2-W*

A T2*-W sequence is very susceptible to external magnetic field inhomogeneities. Gas interfaces, soft tissue mineralization, fibrous tissue, and certain blood degradation products (eg, methemoglobin) cause magnetic field inhomogeneities, which appear

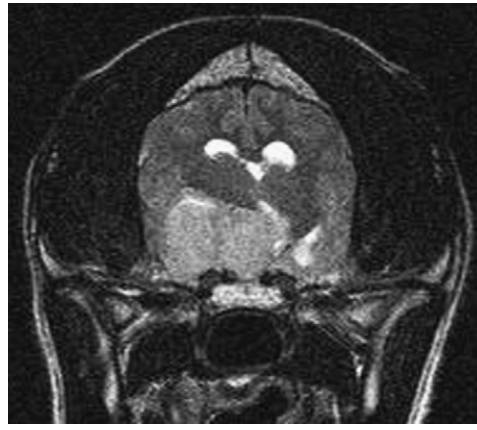

Fig. 2. Transverse T2-W image (same dog as in **Fig. 1**). CSF and mass are hyperintense to brain parenchyma.

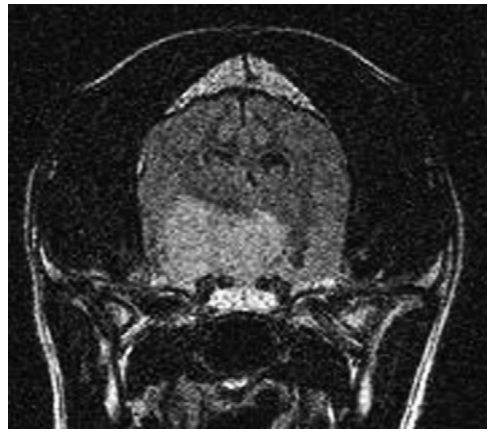

Fig. 3. Transverse FLAIR image (same dog as **Figs. 1** and **2**). The mass remains hyperintense, whereas CSF is attenuated, now appearing as a signal void.

as a signal void (susceptibility artifact) on T2*-W images.[15] T2*-W is most commonly used to identify intracranial hemorrhage and differentiate it from other intracranial lesions (**Fig. 5**).[16] Additional indications include identification of intracranial mineralization (eg, in meningiomas) or abnormal gas pockets (eg, in brain abscesses).

PD-W

PD-W images are acquired by minimizing T1 and T2 relaxation effects on image contrast. Although this sequence is used extensively in musculoskeletal MRI, it only plays a minor role in brain imaging.[2]

DWI and PWI

DWI and PWI are important sequences in imaging of brain tumors[17] and especially, in imaging of cerebral ischemia.[18] DWI is able to demonstrate "Brownian motion" (ie, random movement) of water molecules in brain tissue. As diffusion in biologic

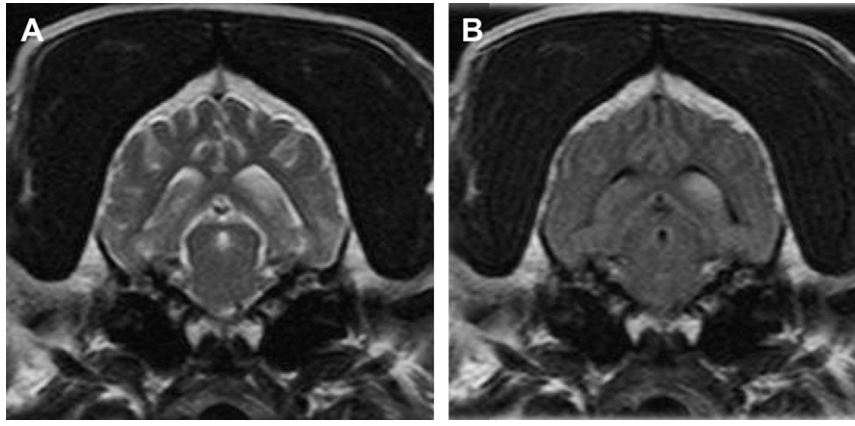

Fig. 4. Transverse T2-W (*A*) and FLAIR (*B*) images in a 9-year-old Labrador retriever with an ischemic infarct as a sequel to intravascular lymphoma. The T2-hyperintense area ventral to the left lateral ventricle is more conspicuous on FLAIR than on T2-W image.

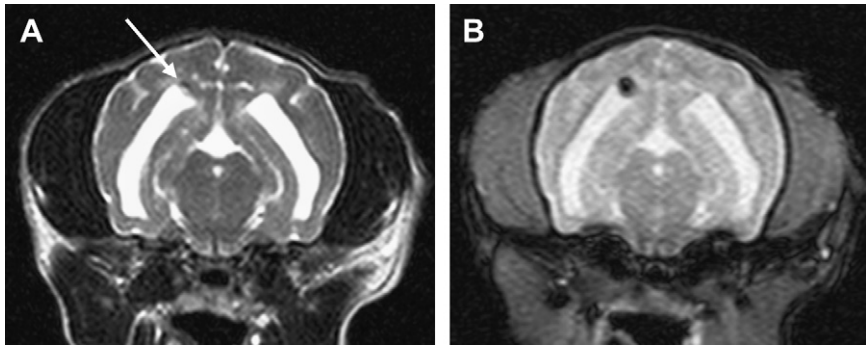

Fig. 5. Transverse T2-W (*A*) and T2*-W (*B*) images in a 13-year-old Yorkshire terrier with presumptive small hemorrhagic infarcts secondary to chronic renal disease and hypertension. On T2-W image, there is a subtle hypointensity associated with the right occipital lobe immediately dorsal to the right lateral ventricle (*arrow*). The lesion is more conspicuous on T2*-W image because of increased sensitivity of this sequence to susceptibility artifacts created by the presence of hemoglobin degradation products.

tissues is not truly random because of the presence of physiologic boundaries (cell membranes and so forth) it is referred to as ''apparent diffusion,'' disturbance of which will appear as abnormal signal intensity on DWI.[19] In acute cerebral ischemia, restricted diffusion occurs secondary to failure of the cell membrane ion pump and subsequent cytotoxic edema. An acute stroke is characterized by marked hyperintensity on a DWI and hypointensity on a synthesized ADC map derived from 2 or more DWI (**Fig. 6**). PWI allows estimation of blood volume passing through the capillary bed per unit of time. This is most commonly accomplished by tracing the passage of a bolus of contrast agent through the cerebral vasculature.[19] Perfusion imaging is often used in combination with DWI in patients with acute ischemic stroke, where the difference between diffusion and perfusion abnormalities provides a measure of the ischemic penumbra (area of reversible ischemia that can be salvaged if blood flow is re-established promptly).

STIR and FatSat

Both techniques result in suppression of signal from fat, which makes them highly valuable in orthopedic and spinal imaging.[4,20] They are not commonly used in brain

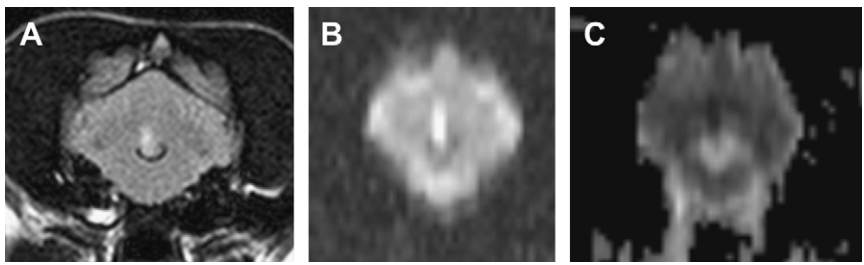

Fig. 6. Transverse FLAIR image (*A*), DWI (*B*), and ADC map (*C*) of a 5-year-old Shi Tzu with a presumptive ischemic infarct. There is a small wedge-shaped hyperintensity within the cerebellum dorsal to the fourth ventricle on FLAIR image, which remains hyperintense on DWI and appears hypointense on the ADC map indicating restricted diffusion. Hyperintense material in the dependent part of the right tympanic bulla is consistent with otitis media (*Courtesy of* Dr Andrea Matthews, University of Tennessee, Knoxville, TN).

imaging but may be considered in select cases, for example, to differentiate a contrast-enhancing lesion from normal tissue, such as bone marrow fat.

Ultrafast SE Techniques

These sequences are heavily T2-W and can be used to image noncirculating liquid structures (eg, pancreatobiliary tract, CSF-filled spaces) (**Fig. 7**).[21,22] "Quick-brain" MR imaging was initially introduced as an alternative technique to CT scanning for assessing children with hydrocephalus. Other indications in humans include macrocephaly, Chiari malformation, intracranial cysts, screening before lumbar puncture, screening for congenital anomalies, and trauma.[23]

MRA

Evaluation of the intracranial circulation in humans provides valuable information in the diagnosis and prognosis of various abnormalities, such as aneurysms, arterial and venous steno-occlusive diseases, inflammatory arterial diseases, and congenital vascular abnormalities.[24] Conventional MRA is usually performed by demonstrating flow-related enhancement (time-of-flight MRA) or demonstrating phase shifts of moving spins (phase shift MRA). Contrast-enhanced MRA is considered superior to conventional MRA.[25] Although intracranial vascular abnormalities are infrequently reported in the veterinary literature, MRA might be considered as a quick and low-risk procedure to evaluate intracranial vessels.[15,26]

High-resolution Sequences

Acquisition of high-resolution images can be helpful in select cases, for example, when detailed evaluation of the inner ear[27] or pituitary gland[28] is required (**Fig. 8**). Specific 3-dimensional (3D) sequences allow acquisition of slices less than 1 mm thick, and they have the added advantage of providing a dataset for 2D and 3D reconstructions without needing to acquire additional imaging planes.

Dynamic Studies

In human medicine, dynamic MRI studies of the brain are performed for assessment of cerebral perfusion[19] and evaluation of brain tumors.[29] A protocol for dynamic MRI of

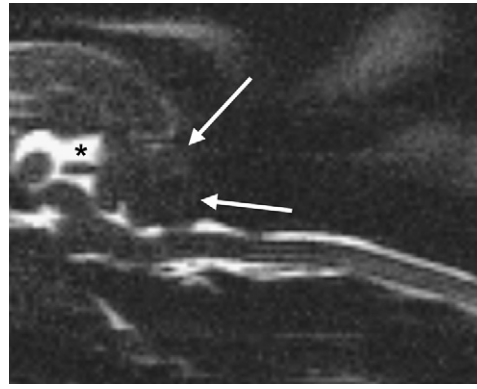

Fig. 7. Sagittal ultrafast heavily T2-W SE image of the caudal head/cranial cervical spine in a Cavalier King Charles Spaniel with mild Chiari-like malformation. There is attenuation of the subarachnoid space caudal to the cerebellum (*arrows*), indicating crowding of the caudal cranial fossa. Mild ventriculomegaly and mild dilation of the quadrigeminal cistern (*) are also noted.

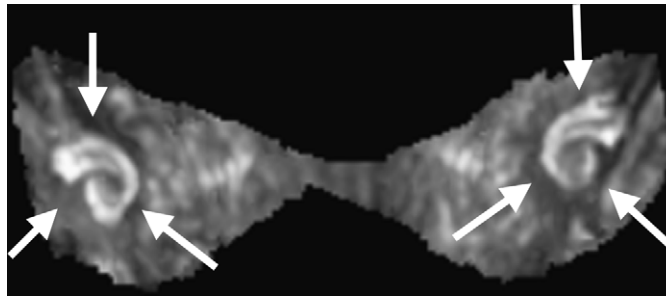

Fig. 8. High resolution 3-dimensional image of the inner ear (*arrows*) in a normal 11-year-old Jack Russell terrier.

the pituitary gland in dogs has been described,[30] which may aid in the diagnosis in pituitary microadenomas.

CONTRAST MEDIA IN MRI

MRI contrast agents most commonly used in veterinary medicine are gadolinium-based.[31] Contrast medium is administered at a dose of 0.1 mmol/kg, which may be increased to improve detection of poorly enhancing lesions. Enhancement is seen if a lesion is vascularized and has disrupted the blood-brain barrier. Gadolinium-based contrast media mostly affect T1 relaxation and therefore enhancing lesions appear hyperintense on T1-W images. Certain normal intracranial structures outside of the blood brain barrier, such as the pituitary gland, choroid plexus, and blood vessels, show physiologic contrast uptake. Although nephrogenic systemic fibrosis has been reported as a serious complication after administration of gadolinium-based contrast agents in humans,[32] adverse systemic effects have not been described in cats[33] or dogs.[34]

APPROACH TO THE MR EXAMINATION OF THE BRAIN

Many disorders of the brain can result in similar MR findings, and some intracranial abnormalities can be detected as incidental findings unrelated to a patient's clinical presentation. Therefore, familiarity with signalment (species, breed, sex, and age) and pertinent history (clinical signs, time of onset of clinical signs, course of disease, and concurrent or previous diseases) are crucial when evaluating brain MRI scans. Intracranial lesions may be extra-axial (ie, originating outside actual brain parenchyma) or intra-axial (originating from brain parenchyma).[16,35,36] Differential diagnoses for extra-axial lesions include certain neoplastic (eg, meningioma, nasal tumor, and so forth), inflammatory (eg, meningitis), and traumatic lesions (eg, epidural/subdural hematoma). Differential diagnoses for solitary intra-axial lesions include neoplasia, hematoma, cyst, abscess/granuloma, and infarct. Although inflammatory brain diseases usually manifest as multifocal lesions, solitary masses may be encountered on occasion. Masses in specific locations may allow a presumptive diagnosis of certain tumor types (eg, pituitary tumors, nerve sheath tumors, medulloblastoma, and so forth). Differential diagnoses for multifocal brain lesions include metabolic/toxic brain disease, inflammatory brain disease, infarcts, and certain intracranial neoplasms (lymphoma, disseminated histiocytic sarcoma, metastases, and occasionally, meningiomas).

ASSOCIATED FINDINGS IN INTRACRANIAL DISEASE

Various pathologic sequelae can be associated with various brain diseases, including hydrocephalus, vasogenic edema, mass effect, brain herniation, and hemorrhage. Hemorrhage will be covered in the second companion article.

Hydrocephalus

Hydrocephalus is defined as abnormal accumulation of cerebrospinal fluid within the cranium.[37] It is a multifactorial disorder that can be classified in various ways:

1. Location:
   - Ventricular system (internal hydrocephalus) versus subarachnoid space (external hydrocephalus)
2. Etiology:
   - Congenital versus acquired
   - Obstructive versus nonobstructive
     - Obstructive hydrocephalus: blockage of CSF flow, for example, secondary to an intracranial space-occupying lesion or congenital stenosis of mesencephalic aqueduct or lateral apertures
     - Compensatory hydrocephalus: decreased volume of brain parenchyma, for example, following trauma or infarction (Hydrocephalus ex vacuo)
     - Decreased resorption (secondary to inflammatory processes or due to underdevelopment of arachnoid villi) or increased production (seen in choroid plexus tumors) of CSF (very rare)
3. Morphology:
   - Communicating (communication between the ventricular system and subarachnoid space) versus noncommunicating (no communication between the ventricular system and subarachnoid space)
4. Pressure:
   - Hypertensive (increased pressure within dilated CSF-filled space, for example, secondary to obstruction) versus normotensive (eg, hydrocephalus ex vacuo)

MRI findings in hydrocephalus include dilation of one or more ventricles or dilation of the subarachnoid space.[36,38] In most cases, abnormal CSF accumulation appears hyperintense on T2-W images, hypointense on T1-W images, and attenuated on FLAIR. If CSF contains abnormal cells or protein (eg, in cases of inflammation or intraventricular hemorrhage), altered signal intensity may be observed. Hypertensive hydrocephalus may be associated with periventricular edema characterized by periventricular T2 hyperintensity,[39] which is most obvious on FLAIR images (**Fig. 9**).[40] Depending on cause, potential concurrent findings in cases of hydrocephalus include other congenital anomalies, an intracranial mass, and trauma. Imaging diagnoses of pathologic hydrocephalus can be challenging. In one study describing ultrasound evaluation of canine lateral ventricles, normal lateral ventricular height was reported to be 0% to 14% of dorsoventral height of the cerebral hemisphere, moderate ventricular enlargement was defined as 15% to 25% of ventricular height to the cerebral hemisphere, and more than 25% was considered consistent with severe ventricular enlargement.[41] However, ventriculomegaly and ventricular asymmetry are common findings in asymptomatic animals and may or may not represent a clinically significant change.[42–46] Progressive dilation of ventricles and subarachnoid space are also anticipated findings with increasing age.[47,48] Therefore, imaging diagnosis, especially of mild ventricular or subarachnoid space dilation, should be judged in light of clinical presentation.

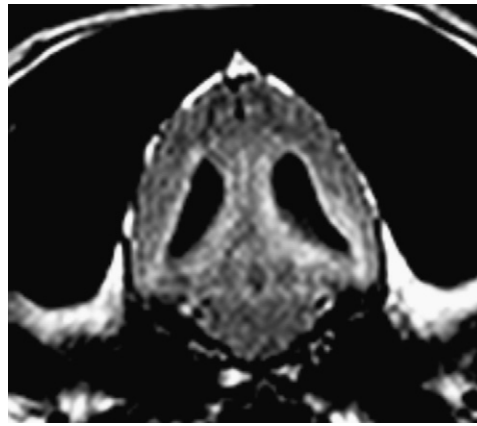

Fig. 9. Transverse FLAIR image of a dog with obstructive hydrocephalus demonstrating periventricular T2 hyperintensity (edema).

Vasogenic Edema

Vasogenic brain edema may be seen concurrently with several intracranial diseases. Under normal circumstances, exchange of substances between the blood and the brain is limited by the blood-brain barrier. Damage to brain capillaries results in leakage of fluid into the extracellular space (vasogenic edema). The edema migrates along the white matter fiber tracts and may create a mass effect. Vasogenic edema appears hyperintense on T2-W MR images and hypointense on T1-W images, and it often has the same signal intensity as the lesion causing the edema (**Fig. 10**A). After contrast medium administration, gadolinium leaks out of damaged capillaries, resulting in increased signal intensity of the lesion responsible for the edema, whereas the edema remains hypointense on postcontrast T1-W images (**Fig. 10**B).[2,9]

Mass Effect

Space-occupying lesions within the cranial vault (eg, tumor, abscess/granuloma, edema, hydrocephalus) are commonly associated with a mass effect, which is indicated by displacement of the falx cerebri or compression of the ventricular system.[49]

Brain Herniation

Increase in intracranial pressure (eg, due to an intracranial mass) can lead to compression and displacement of brain parenchyma.[50–52] Foramen magnum herniation (herniation of the caudal portion of the cerebellum into and through the foramen magnum) and caudal transtentorial herniation (displacement of portions of the cerebral cortex ventral to the tentorium cerebelli) are most common and are best evaluated on sagittal images (**Fig. 11**).

Seizures and Cerebral Necrosis

The relationship between seizures and brain injury remains diagnostically challenging.[37] In human patients, it has been shown that severe seizure activity causes reversible changes in certain areas of the brain, such as the neocortex, hippocampus, and amygdala.[53,54] Brain parenchymal changes, including edema, neovascularization, reactive astrocytosis, and acute neuronal necrosis, have been reported in dogs with

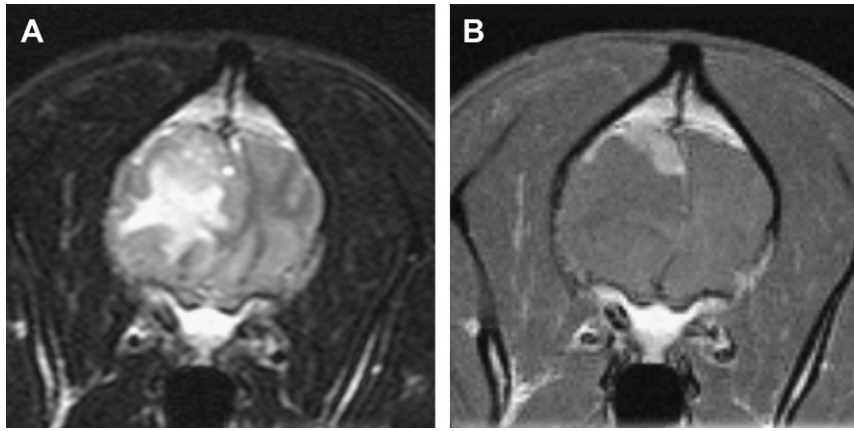

Fig. 10. Vasogenic edema in a dog with an intracranial mass, presumptive meningioma. On T2-W image (*A*) there is extensive hyperintensity associated with the white-matter tracts of the right cerebral hemisphere. On T1-W postcontrast image (*B*) there is homogenous enhancement of a plaque-like mass extending ventral to the right frontal bone and coursing ventrally with the falx cerebri. Edematous brain parenchyma appears hypointense on this image, and mass effect is indicated by leftward displacement of the falx.

seizures.[55] These lesions appeared as unilateral or bilateral T2 hyperintense and T1 hypointense foci, with variable contrast enhancement associated with piriform or temporal lobes (**Fig. 12**). Changes resolved on recheck examination, indicating that they most probably represented sequelae to seizures rather than their underlying cause. Cerebral cortical necrosis (polioencephalomalacia) appearing as increased T1 and T2 signal intensity of the gray matter of temporal and parietal lobes with mild contrast enhancement has been reported in a dog with seizures.[56] Signal characteristics were attributed to large numbers of fat-containing macrophages found within these areas on histopathologic examination. Necrosis of hippocampus and piriform lobes in cats with seizures has been described as bilaterally symmetric T2 hyperintensity of hippocampus and piriform lobes with variable contrast enhancement.[57,58] In these studies, structural brain damage was thought to be the underlying cause of seizures. In some cases, it may not be possible to determine whether brain changes

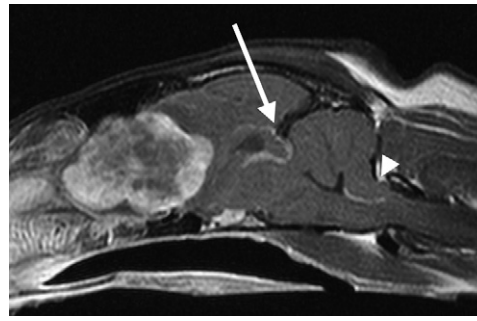

Fig. 11. Sagittal T1-W post contrast image of the brain in an 8-year-old cat with a large intracranial mass and secondary foramen magnum (*arrowhead*) and subtentorial (*arrow*) brain herniation.

Fig. 12. Transverse FLAIR image of a 9-year-old boxer presented with seizures. There are asymmetric T2 hyperintense areas associated with the piriform lobes and hippocampus bilaterally.

found on MRI or histopathology represent the underlying cause or the result of seizures.[37,56]

CONGENITAL BRAIN DISORDERS

Forebrain (Telencephalon and Diencephalon)

Imaging findings in congenital abnormalities of the cerebrum are infrequently reported in the veterinary literature. Congenital hydrocephalus is most commonly seen in toy and brachycephalic breed dogs and appears as dilation of the ventricular system of variable severity.[59] In hydranencephaly, there is near complete destruction or lack of development of the neocortex.[37] MRI findings have been described in 2 kittens with hydranencephaly attributed to intrauterine parvovirus infection.[60] Affected animals showed reduction of size of one or both cerebral cortices to a thin mantle surrounding a large, centrally located cavity. Porencephaly appears as cystic cavities in the cerebrum due to cell destruction or failure of development.[37] These cavities show signal typical of CSF on MRI and may communicate with ventricles or the subarachnoid space.[40] Lissencephaly is a brain malformation characterized by a paucity of hypoplastic gyri and thickening of the cerebral cortex. MRI findings in 2 Lhasa Apso dogs with lissencephaly included a smooth cerebral surface and a thick neocortex with absence of the corona radiata.[61] Agenesis of the corpus callosum has been reported to result in abnormal appearance of the cingulate gyrus.[40] Holoprosencephaly is characterized by an absence or reduction in size of midline prosencephalic structures (corpus callosum, septum pellucidum, septal nuclei, fornix, and optic nerves), incomplete separation of normally paired forebrain structures (lateral ventricles, cingulate gyri, and caudate nuclei), and hydrocephalus.[62] Protrusion of meninges and meninges along with brain tissue through a calvarial defect are termed meningocele and meningoencephalocele, respectively.[37] MR diagnoses of a frontoethmoidal meningoencephalocele in a German shepherd dog[63] and an ethmoidal encephalocele in a mixed-breed dog[64] have been reported. Rathke cleft cysts are

pituitary cysts containing mucoid or, less commonly, serous fluid and cellular debris, and they appear as cystic lesions in the middle cranial fossa, which are hypointense on T1-W images, hyperintense on T2-W images, may show mild ring enhancement, and may not suppress on FLAIR because of composition of fluid.[40,65]

Midbrain and Hindbrain (Mesencephalon, Metencephalon, Myelencephalon)

Intracranial intra-arachnoid cysts are considered developmental anomalies that arise from splitting/duplication of the arachnoidea in early embryonic development and occur in close association with an intracranial arachnoid cistern. Quadrigeminal cistern cysts dorsal to the quadrigeminal plate are most common, but cerebellomedullary cistern cysts have also been reported.[66,67] Intracranial intra-arachnoid cysts contain fluid isointense to CSF, with attenuation on FLAIR and no evidence of contrast enhancement (**Fig. 13**). Hemorrhage into intracranial intra-arachnoid cysts may change the signal intensity.[68] Quadrigeminal cysts are of variable significance and are frequently incidental.[69] In one study, occipital lobe compression greater than 14% by the cyst on median-sagittal image was always associated with clinical signs, whereas no association was found between degree of cerebellar compression and clinical signs.[66]

Chiari malformations are a group of structural defects involving brainstem, cerebellum, upper spinal cord, and surrounding bony structures in humans.[70] Secondary formation of a cystic cavity within the cervical spinal cord parenchyma or dilation of the central canal (syringohydromyelia) are common. A disorder similar to Chiari type I malformation in humans termed ''Chiari-like malformation and syringomyelia'' has been reported in dogs.[71–73] Cavalier King Charles spaniels are most commonly affected, but the disease is seen in various breeds and can be found in symptomatic and asymptomatic animals.[74] The condition is characterized by crowding of the caudal fossa, resulting in attenuation of the subarachnoid space surrounding the cerebellum, compression and, in severe cases, herniation of the cerebellum into or through the foramen magnum, best demonstrated on T2-W median-sagittal image. Additional findings include a focal bending of the cranial aspect of the spinal cord, hydrocephalus and syringohydromyelia (**Fig. 14**).[75,76]

Cerebellar hypoplasia can occur as a primary developmental defect or secondary to in utero or perinatal viral infection, most commonly parvovirus.[37,77] MRI diagnosis is

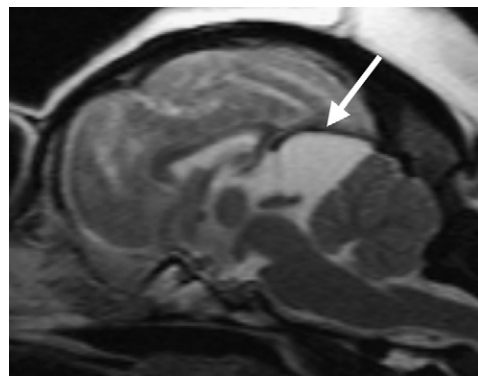

Fig. 13. Sagittal T2-W image of the brain in a 10-year-old Pekingese presented with cervical intervertebral disk extrusion, demonstrating an incidental quadrigeminal cistern cyst rostral to the cerebellum (*arrow*).

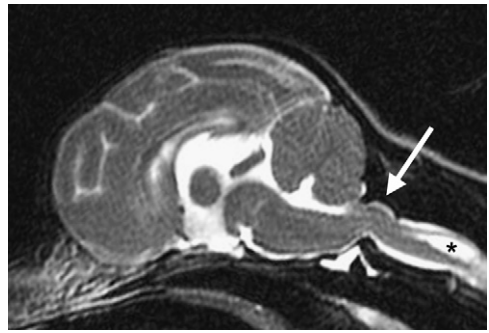

Fig. 14. Sagittal T2-W image of a Cavalier King Charles spaniel with Chiari-like malformation and syringomyelia. There is crowding of the caudal fossa resulting in attenuation of the subarachnoid space and compression of the cerebellum, dorsal angulation of the spinal cord at the level of the foramen magnum and odontoid process of C2 (*arrow*), mild hydrocephalus, and syringohydromyelia (*).

best made on sagittal T2-W image. The cerebellum may appear small, with increased CSF signal noted around and extending into the folia.[40] Subtotal agenesis of the cerebellum in a Shi Tzu was characterized by absence of most of the cerebellum with normal size of the caudal fossa.[78] Isolated hypoplasia of the cerebellar vermis has been reported in a miniature Schnauzer.[79] In 2 kittens, MR findings of cerebellar cyst and the small size of the cerebellum were attributed to intrauterine parvovirus infection.[60] Congenital cerebellar abnormalities may not always be apparent on MRI examination. No abnormalities were detected in Coton de Tulear dogs with neonatal cerebellar ataxia.[80] Differentiation of true cerebellar hypoplasia from degenerative disease (cerebellar atrophy, abiotrophy, and degeneration) is not possible solely based on imaging findings.

The Dandy-Walker malformation complex in human patients refers to a group of congenital central nervous system anomalies that primarily involve the cerebellum and adjacent tissues.[81] The primary abnormality is partial or complete absence of

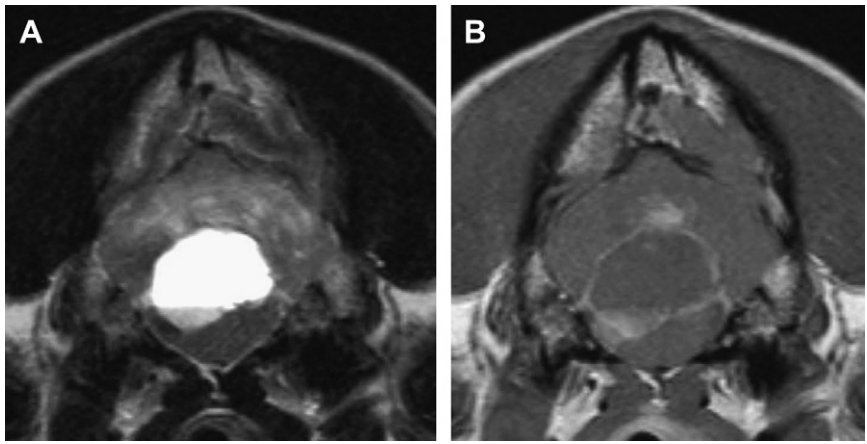

Fig. 15. Epidermoid cyst in a 3-year-old dog. Transverse T2-W image (*A*) of the caudal fossa shows a heterogeneous mass consisting of a cystic component dorsally and solid component ventrally, with ring and solid component enhancement present on T1-W image following contrast medium administration (*B*).

the cerebellar vermis and cystic dilation of the fourth ventricle. Additional abnormalities, such as hydrocephalus, stenosis of the mesencephalic aqueduct, and absence of the corpus callosum, may be present.[37] MRI findings in a golden retriever with Dandy-Walker malformation included generalized ventricular enlargement, extension of the cystic fourth ventricle into the supratentorial space with displacement of the occipital lobes, absence of cerebellar vermis, reduced size of the cerebellar hemispheres, widening and irregular gyrification of cerebral sulci, and absence of the corpus callosum.[82]

A case of cerebellar ependymal cyst has been reported in a Staffordshire terrier.[83] On MRI, the area of the cerebellum was almost completely replaced by a fluid collection independent of the fourth ventricle and isointense to CSF.

Intracranial epidermoid and dermoid cysts are benign space-occupying lesions that originate from remnants of ectodermal tissue because of defects of neural tube closure.[37] They are often located in the cerebellopontine angle or the fourth ventricle. Signal intensity is variable and dependent on cyst content. Cysts with a high lipid content appear hyperintense on T1-W and T2-W images,[84] whereas cysts with lower lipid content appear hypointense on T1-W images and hyperintense on T2-W images.[85,86] Dermoid cysts containing adnexa (eg, hair) may show suspended low intensity foci in all sequences.[84] Cysts often contain protein and keratin and therefore, do not attenuate on FLAIR.[86] They usually do not show contrast enhancement, although ring enhancement may occasionally be noted (**Fig. 15**).

REFERENCES

1. Thomson CE, Kornegay JN, Burn RA, et al. Magnetic resonance imaging - a general overview of principles and examples in veterinary neurodiagnosis. Vet Radiol Ultrasound 1993;34(1):2–17.
2. Tidwell AS, Jones JC. Advanced imaging concepts: a pictorial glossary of CT and MRI technology. Clin Tech Small Anim Pract 1999;14(2):65–111.
3. McRobbie DW, Moore EA, Graves MJ, et al. MRI - from picture to Proton. Cambridge (UK): University Press; 2003.
4. Westbrook C, Kaut Roth C, Talbot J. MRI in practice. Oxford (UK): Blackwell Publishing Ltd; 2005.
5. Pooley RA. AAPM/RSNA physics tutorial for residents: fundamental physics of MR imaging. Radiographics 2005;25(4):1087–99.
6. Faulkner W. Rad tech's guide to MRI: basic physics, instrumentation, and quality control. Malden (MA): Blackwell Science, Inc.; 2002.
7. Mikulis DJ, Roberts TP. Neuro MR: protocols. J Magn Reson Imaging 2007;26(4): 838–47.
8. Roberts TP, Mikulis D. Neuro MR: principles. J Magn Reson Imaging 2007;26(4): 823–37.
9. Tidwell AS. Principles of computed tomography and magnetic resonance imaging. In: Thrall DE, editor. Textbook of veterinary diagnostic radiology. 5th edition. St. Louis (MO): Saunders Elsevier; 2007. p. 50–77.
10. Sage JE, Samii VF, Abramson CJ, et al. Comparison of conventional spin-echo and fast spin-echo magnetic resonance imaging in the canine brain. Vet Radiol Ultrasound 2006;47(3):249–53.
11. Benigni L, Lamb CR. Comparison of fluid-attenuated inversion recovery and T2-weighted magnetic resonance images in dogs and cats with suspected brain disease. Vet Radiol Ultrasound 2005;46(4):287–92.

12. Cherubini GB, Platt SR, Howson S, et al. Comparison of magnetic resonance imaging sequences in dogs with multi-focal intracranial disease. J Small Anim Pract 2008;49(12):634–40.
13. Essig M, Bock M. Contrast optimization of fluid-attenuated inversion-recovery (FLAIR) MR imaging in patients with high CSF blood or protein content. Magn Reson Med 2000;43(5):764–7.
14. Falzone C, Rossi F, Calistri M, et al. Contrast-enhanced fluid-attenuated inversion recovery vs. contrast-enhanced spin echo T1-weighted brain imaging. Vet Radiol Ultrasound 2008;49(4):333–8.
15. Wessmann A, Chandler K, Garosi L. Ischaemic and haemorrhagic stroke in the dog. Vet J 2009;180(3):290–303.
16. Robertson ID. Magnetic resonance imaging features of brain disease in small animals. In: Thrall DE, editor. Textbook of veterinary diagnostic radiology. 5th edition. St. Louis (MO): Saunders Elsevier; 2007. p. 142–59.
17. Pomper MG, Port JD. New techniques in MR imaging of brain tumors. Magn Reson Imaging Clin N Am 2000;8(4):691–713.
18. Roberts TP, Rowley HA. Diffusion weighted magnetic resonance imaging in stroke. Eur J Radiol 2003;45(3):185–94.
19. Crawley AP, Poublanc J, Ferrari P, et al. Basics of diffusion and perfusion MRI. Appl Radiol 2003;32(4):13–23.
20. Scarabino T, Giannatempo GM, Popolizio T, et al. [Fast spin echo imaging of vertebral metastasis: comparison of fat suppression techniques (FSE-CHESS, STIR-FSE)]. Radiol Med 1996;92(3):180–5 [in Italian].
21. Pease A, Sullivan S, Olby N, et al. Value of a single-shot turbo spin-echo pulse sequence for assessing the architecture of the subarachnoid space and the constitutive nature of cerebrospinal fluid. Vet Radiol Ultrasound 2006;47(3):254–9.
22. Tang Y, Yamashita Y, Takahashi M. Ultrafast T2-weighted imaging of the abdomen and pelvis: use of single shot fast spin-echo imaging. J Magn Reson Imaging 1998;8(2):384–90.
23. Missios S, Quebada PB, Forero JA, et al. Quick-brain magnetic resonance imaging for nonhydrocephalus indications. J Neurosurg Pediatr 2008;2(6): 438–44.
24. Ozsarlak O, Van Goethem JW, Maes M, et al. MR angiography of the intracranial vessels: technical aspects and clinical applications. Neuroradiology 2004;46(12): 955–72.
25. Anzalone N. Contrast-enhanced MRA of intracranial vessels. Eur Radiol 2005; 15(Suppl 5):E3–10.
26. Sager M, Assheuer J, Trummler H, et al. Contrast-enhanced magnetic resonance angiography (CE-MRA) of intra- and extra-cranial vessels in dogs. Vet J 2009; 179(1):92–100.
27. Garosi LS, Dennis R, Penderis J, et al. Results of magnetic resonance imaging in dogs with vestibular disorders: 85 cases (1996–1999). J Am Vet Med Assoc 2001;218(3):385–91.
28. van der Vlugt-Meijer RH, Meij BP, Voorhout G. Thin-slice three-dimensional gradient-echo magnetic resonance imaging of the pituitary gland in healthy dogs. Am J Vet Res 2006;67(11):1865–72.
29. Senturk S, Oguz KK, Cila A. Dynamic contrast-enhanced susceptibility-weighted perfusion imaging of intracranial tumors: a study using a 3T MR scanner. Diagn Interv Radiol 2009;15(1):3–12.
30. Graham JP, Roberts GD, Newell SM. Dynamic magnetic resonance imaging of the normal canine pituitary gland. Vet Radiol Ultrasound 2000;41(1):35–40.

31. Kuriashkin IV, Losonsky JM. Contrast enhancement in magnetic resonance imaging using intravenous paramagnetic contrast media: a review. Vet Radiol Ultrasound 2000;41(1):4–7.
32. Bhave G, Lewis JB, Chang SS. Association of gadolinium based magnetic resonance imaging contrast agents and nephrogenic systemic fibrosis. J Urol 2008; 180(3):830–5.
33. Pollard RE, Puchalski SM, Pascoe PJ. Hemodynamic and serum biochemical alterations associated with intravenous administration of three types of contrast media in anesthetized cats. Am J Vet Res 2008;69(10):1274–8.
34. Pollard RE, Puchalski SM, Pascoe PJ. Hemodynamic and serum biochemical alterations associated with intravenous administration of three types of contrast media in anesthetized dogs. Am J Vet Res 2008;69(10):1268–73.
35. Kraft SL, Gavin PR. Intracranial neoplasia. Clin Tech Small Anim Pract 1999;14(2): 112–23.
36. Thomas WB. Nonneoplastic disorders of the brain. Clin Tech Small Anim Pract 1999;14(3):125–47.
37. Summers BA, Cummings JF, de Lahunta A. Veterinary neuropathology. St. Louis (MO): Mosby; 1995.
38. Dewey CW, Coates JR, Ducote JM, et al. External hydrocephalus in two cats. J Am Anim Hosp Assoc 2003;39(6):567–72.
39. Drake JM, Potts DG, Lemaire C. Magnetic resonance imaging of silastic-induced canine hydrocephalus. Surg Neurol 1989;31(1):28–40.
40. Matiasek LA. Malformations of the brain and neurocranium - magnetic resonance imaging features. Newmarket: European Association of Veterinary Diagnostic Imaging (EAVDI). EAVDI Yearbook 2008. p. 1–30.
41. Spaulding KA, Sharp NJH. Ultrasonographic imaging of the lateral cerebral ventricles in the dog. Vet Radiol 1990;31(2):59–64.
42. De Haan C, Kraft SL, Gavin PR, et al. Normal variation in size of the lateral ventricles of the labrador retriever dog as assessed by magnetic resonance imaging. Vet Radiol Ultrasound 1994;35(2):83–6.
43. Kii S, Uzuka Y, Taura Y, et al. Magnetic resonance imaging of the lateral ventricles in beagle-type dogs. Vet Radiol Ultrasound 1997;38(6):430–3.
44. Vite CH, Insko EK, Schotland HM, et al. Quantification of cerebral ventricular volume in English bulldogs. Vet Radiol Ultrasound 1997;38(6):437–43.
45. Vullo T, Korenman E, Manzo RP, et al. Diagnosis of cerebral ventriculomegaly in normal adult beagles using quantitative MRI. Vet Radiol Ultrasound 1997;38(4): 277–81.
46. Esteve-Ratsch B, Kneissl S, Gabler C. Comparative evaluation of the ventricles in the Yorkshire Terrier and the German Shepherd dog using low-field MRI. Vet Radiol Ultrasound 2001;42(5):410–3.
47. Hasegawa D, Yayoshi N, Fujita Y, et al. Measurement of interthalamic adhesion thickness as a criteria for brain atrophy in dogs with and without cognitive dysfunction (dementia). Vet Radiol Ultrasound 2005;46(6):452–7.
48. Kimotsuki T, Nagaoka T, Yasuda M, et al. Changes of magnetic resonance imaging on the brain in beagle dogs with aging. J Vet Med Sci 2005;67(10):961–7.
49. Thomas WB, Wheeler SJ, Kramer R, et al. Magnetic resonance imaging features of primary brain tumors in dogs. Vet Radiol Ultrasound 1996;37(1):20–7.
50. Kornegay JN, Oliver JE Jr, Gorgacz EJ. Clinicopathologic features of brain herniation in animals. J Am Vet Med Assoc 1983;182(10):1111–6.
51. Bagley RS. Pathophysiologic sequelae of intracranial disease. Vet Clin North Am Small Anim Pract 1996;26(4):711–33.

52. Walmsley GL, Herrtage ME, Dennis R, et al. The relationship between clinical signs and brain herniation associated with rostrotentorial mass lesions in the dog. Vet J 2006;172(2):258–64.
53. Aykut-Bingol C, Tekin S, Ince D, et al. Reversible MRI lesions after seizures. Seizure 1997;6(3):237–9.
54. Chan S, Chin SS, Kartha K, et al. Reversible signal abnormalities in the hippocampus and neocortex after prolonged seizures. AJNR Am J Neuroradiol 1996; 17(9):1725–31.
55. Mellema LM, Koblik PD, Kortz GD, et al. Reversible magnetic resonance imaging abnormalities in dogs following seizures. Vet Radiol Ultrasound 1999;40(6): 588–95.
56. Mariani CL, Platt SR, Newell SM, et al. Magnetic resonance imaging of cerebral cortical necrosis (polioencephalomalacia) in a dog. Vet Radiol Ultrasound 2001;42(6):524–31.
57. Fatzer R, Gandini G, Jaggy A, et al. Necrosis of hippocampus and piriform lobe in 38 domestic cats with seizures: a retrospective study on clinical and pathologic findings. J Vet Intern Med 2000;14(1):100–4.
58. Schmied O, Scharf G, Hilbe M, et al. Magnetic resonance imaging of feline hippocampal necrosis. Vet Radiol Ultrasound 2008;49(4):343–9.
59. Dewey CW. Encephalopathies: disorders of the brain. In: Dewey CW, editor. A practical guide to canine and feline neurology. Ames (IA): Iowa State Press; 2003. p. 99–178.
60. Sharp NJ, Davis BJ, Guy JS, et al. Hydranencephaly and cerebellar hypoplasia in two kittens attributed to intrauterine parvovirus infection. J Comp Pathol 1999; 121(1):39–53.
61. Saito M, Sharp NJ, Kortz GD, et al. Magnetic resonance imaging features of lissencephaly in 2 Lhasa Apsos. Vet Radiol Ultrasound 2002;43(4):331–7.
62. Sullivan SA, Harmon BG, Purinton PT, et al. Lobar holoprosencephaly in a Miniature Schnauzer with hypodipsic hypernatremia. J Am Vet Med Assoc 2003; 223(12):1783–7.
63. Kärkkäinen M. Low- and high-field strength magnetic resonance imaging to evaluate the brain in one normal dog and two dogs with central nervous system disease. Vet Radiol Ultrasound 1995;36(6):528–32.
64. Jeffery N. Ethmoidal encephalocoele associated with seizures in a puppy. J Small Anim Pract 2005;46(2):89–92.
65. Hasegawa D, Uchida K, Kobayashi T, et al. Imaging diagnosis - Rathke's cleft cyst. Vet Radiol Ultrasound 2009;50(3):298–300.
66. Matiasek LA, Platt SR, Shaw S, et al. Clinical and magnetic resonance imaging characteristics of quadrigeminal cysts in dogs. J Vet Intern Med 2007;21(5):1021–6.
67. Vernau KM, Kortz GD, Koblik PD, et al. Magnetic resonance imaging and computed tomography characteristics of intracranial intra-arachnoid cysts in 6 dogs. Vet Radiol Ultrasound 1997;38(3):171–6.
68. Vernau KM, LeCouteur RA, Sturges BK, et al. Intracranial intra-arachnoid cyst with intracystic hemorrhage in two dogs. Vet Radiol Ultrasound 2002;43(5): 449–54.
69. Duque C, Parent J, Brisson B, et al. Intracranial arachnoid cysts: are they clinically significant? J Vet Intern Med 2005;19(5):772–4.
70. Tubbs RS, Shoja MM, Ardalan MR, et al. Hindbrain herniation: a review of embryological theories. Ital J Anat Embryol 2008;113(1):37–46.
71. Cappello R, Rusbridge C. Report from the Chiari-like malformation and syringomyelia working group round table. Vet Surg 2007;36(5):509–12.

72. Rusbridge C, Greitz D, Iskandar BJ. Syringomyelia: current concepts in pathogenesis, diagnosis, and treatment. J Vet Intern Med 2006;20(3):469–79.
73. Rusbridge C, Knowler SP. Inheritance of occipital bone hypoplasia (Chiari type I malformation) in Cavalier King Charles spaniels. J Vet Intern Med 2004;18(5): 673–8.
74. Couturier J, Rault D, Cauzinille L. Chiari-like malformation and syringomyelia in normal cavalier King Charles spaniels: a multiple diagnostic imaging approach. J Small Anim Pract 2008;49(9):438–43.
75. Lu D, Lamb CR, Pfeiffer DU, et al. Neurological signs and results of magnetic resonance imaging in 40 cavalier King Charles spaniels with Chiari type 1-like malformations. Vet Rec 2003;153(9):260–3.
76. Kitagawa M, Kanayama K, Sakai T. Quadrigeminal cisterna arachnoid cyst diagnosed by MRI in five dogs. Aust Vet J 2003;81(6):340–3.
77. Schatzberg SJ, Haley NJ, Barr SC, et al. Polymerase chain reaction (PCR) amplification of parvoviral DNA from the brains of dogs and cats with cerebellar hypoplasia. J Vet Intern Med 2003;17(4):538–44.
78. Kitagawa M, Kanayama K, Sakai T. Subtotal agenesis of the cerebellum in a dog. Aust Vet J 2005;83(11):680–1.
79. Choi H, Kang S, Jeong S, et al. Imaging diagnosis-cerebellar vermis hypoplasia in a miniature schnauzer. Vet Radiol Ultrasound 2007;48(2):129–31.
80. Coates JR, O'Brien DP, Kline KL, et al. Neonatal cerebellar ataxia in Coton de Tulear dogs. J Vet Intern Med 2002;16(6):680–9.
81. Patel S, Barkovich AJ. Analysis and classification of cerebellar malformations. Am J Neuroradiol 2002;23(7):1074–87.
82. Schmidt MJ, Jawinski S, Wigger A, et al. Imaging diagnosis-Dandy walker malformation. Vet Radiol Ultrasound 2008;49(3):264–6.
83. Wyss-Fluehmann G, Konar M, Jaggy A, et al. Cerebellar ependymal cyst in a dog. Vet Pathol 2008;45(6):910–3.
84. Targett MP, McInnes E, Dennis R. Magnetic resonance imaging of a medullary dermoid cyst with secondary hydrocephalus in a dog. Vet Radiol Ultrasound 1999;40(1):23–6.
85. Platt SR, Graham J, Chrisman CL, et al. Canine intracranial epidermoid cyst. Vet Radiol Ultrasound 1999;40(5):454–8.
86. Steinberg T, Matiasek K, Bruhschwein A, et al. Imaging diagnosis–intracranial epidermoid cyst in a Doberman Pinscher. Vet Radiol Ultrasound 2007;48(3): 250–3.